Performance enhancement of GaN-based flip-chip ultraviolet light-emitting diodes with a RPD AlN nucleation layer on patterned sapphire substrate

B. C. Lin,[1] C. H. Chiu,[1,2,*] C. Y. Lee,[1] H. V. Han,[1] P. M. Tu,[1,2] T. P. Chen,[1] Z. Y. Li,[1] P. T. Lee,[1] C. C. Lin,[3,7] G. C. Chi,[1] C. H. Chen,[4] B. Fan,[4] C. Y. Chang,[5] and H. C. Kuo[1,6]

[1]*Department of Photonics and Institute of Electro-Optical Engineering, National Chiao Tung University, Hsinchu 30010, Taiwan*
[2]*Advanced Optoelectronic Technology Inc., No. 13, Gongye 5th Rd., Hukou Township, Hsinchu County 303, Taiwan*
[3]*Institute of Photonics System National Chiao Tung University, Tainan 71150, Taiwan*
[4]*Optorum Co., Ltd, Saitama-Ken, Japan*
[5]*Institute of Electronics, National Chiao Tung University, Hsinchu 30010, Taiwan*
[6]*hckuo@faculty.nctu.edu.tw*
[7]*chienchunglin@faculty.nctu.edu.tw*
[*]*jim.chiu@aot.com.tw*

Abstract: In this work, flip-chip ultraviolet light-emitting diodes (FCUV-LEDs) on patterned sapphire substrate (PSS) at 375 nm were grown by an atmospheric pressure metal organic chemical vapor deposition (AP-MOCVD). A specialized reactive plasma deposited (RPD) AlN nucleation layer was utilized on the PSS to enhance the quality of the epitaxial layer. By using high-resolution X-ray diffraction, the full-width at half-maximum of the rocking curve shows that the FCUV-LEDs with RPD AlN nucleation layer had better crystalline quality when compared to conventional GaN nucleation samples. From the transmission electron microscopy (TEM) image, it can be observed that the tip and incline portion of the pattern was smooth using the RPD AlN nucleation layer. The threading dislocation densities (TDDs) are reduced from 7×10^7 cm^{-2} to 2.5×10^7 cm^{-2} at the interface between the u-GaN layers for conventional and AlN PSS devices, respectively. As a result, a much higher light output power was achieved. The improvement of light output power at an injection current of 20 mA was enhanced by 30%. Further photoluminescence measurement and numerical simulation confirm such increase of output power can be attributed to the improvement of material quality and light extraction.

OCIS codes: (230.3670) Light-emitting diodes; (230.2090) Electro-optical devices.

References and links

1. S. Nakamura, M. Senoh, N. Iwsa, and S.-I. Nagahama, "High-brightness InGaN blue, green and yellow light-emtting diodes with quantum well structures," Jpn. J. Appl. Phys. **34**(Part 2, No. 7A), L797–L799 (1995).
2. T. Mukai, M. Yamada, and S. Nakamura, "Characteristics of InGaN-based UV/blue/green/amber/red light-emitting diodes," Jpn. J. Appl. Phys. **38**(Part 1, No. 7A), 3976–3981 (1999).
3. Y. C. Chiu, W. R. Liu, C. K. Chang, C. C. Liao, Y. T. Yeh, S. M. Jang, and T. M. Chen, "$Ca_2PO_4Cl:Eu^{2+}$: An intense near-ultraviolet converting blue phosphor for white light-emitting diodes," J. Mater. Chem. **20**(9), 1755–1758 (2010).
4. P. M. Tu, C. Y. Chang, S. C. Huang, C. H. Chiu, J. R. Chang, W. T. Chang, D. S. Wuu, H. W. Zan, C. C. Lin, H. C. Kuo, and C. P. Hsu, "Investigation of efficiency droop for InGaN-based UV light-emitting diodes with InAlGaN barrier," Appl. Phys. Lett. **98**(21), 211107 (2011).
5. Y. S. Tang, S. F. Hu, C. C. Lin, N. C. Bagkar, and R. S. Liu, "Thermally stable luminescence of $KSrPO_4:Eu^{2+}$ phosphor for white light UV light-emitting diodes," Appl. Phys. Lett. **90**(15), 151108 (2007).

#210923 - $15.00 USD Received 25 Apr 2014; revised 19 Jun 2014; accepted 20 Jun 2014; published 17 Jul 2014

6. Y. Narukawa, J. Narita, T. Sakamoto, K. Deguchi, T. Yamada, and T. Mukai, "Ultra-high efficiency white light emitting diodes," Jpn. J. Appl. Phys. **45**(41), L1084–L1086 (2006).
7. S. Nakamura, M. Senoh, S. Nagahama, N. Iwasa, T. Yamada, T. Matsushita, H. Kiyoku, Y. Sugimoto, T. Kozaki, H. Umemoto, M. Sano, and K. Chocho, "InGaN/GaN/AlGaN-based laser diodes with modulation-doped strained-layer structures grown on an epitaxially laterally overgrown GaN substrate," Appl. Phys. Lett. **72**(2), 211–213 (1998).
8. S. W. Feng, Y. C. Cheng, Y. Y. Chung, C. C. Yang, Y.-S. Lin, C. Hsu, K.-J. Ma, and J.-I. Chyi, "Impact of localized states on the recombination dynamics in InGaN/GaN quantum well structures," J. Appl. Phys. **92**(8), 4441–4448 (2002).
9. S. D. Lester, F. A. Ponce, M. G. Craford, and D. A. Steigerwald, "High dislocation densities in high-efficiency GaN-based light-emitting diodes," Appl. Phys. Lett. **66**(10), 1249–1251 (1995).
10. T. Wang, Y. H. Lin, Y. B. Lee, Y. Izumi, J. P. Ao, J. Bai, H. D. Li, and S. Sakai, "Fabrication of high performance of AlGaN/GaN-based UV light-emitting diodes," J. Cryst. Growth **235**(1-4), 177–182 (2002).
11. D. Kapolnek, S. Keller, R. Vetury, R. D. Underwood, P. Kozodoy, S. P. DenBaars, and U. K. Mishra, "Anisotropic epitaxial lateral growth in GaN selective are epitaxy," Appl. Phys. Lett. **71**(9), 1204–1206 (1997).
12. T. S. Zheleva, O.-H. Nam, M. D. Bremser, and R. F. Davis, "Dislocation density reduction via lateral epitaxy in selectively grown GaN structures," Appl. Phys. Lett. **71**(17), 2472–2474 (1997).
13. D. M. Follstaedt, P. P. Provencio, N. A. Missert, C. C. Mitchell, D. D. Koleske, A. A. Allerma, and C. I. H. Ashby, "Minimizing threading dislocations by redirection during cantilever epitaxial growth of GaN," Appl. Phys. Lett. **81**(15), 2758–2760 (2002).
14. M. H. Lo, P. M. Tu, C. H. Wang, Y. J. Cheng, C. W. Hung, S. C. Hsu, H. C. Kuo, H. W. Zan, S. C. Wang, C. Y. Chang, and C. M. Liu, "Defect selective passivation in GaN epitaxial growth and its application to light emitting diodes," Appl. Phys. Lett. **95**(21), 211103 (2009).
15. A. Sakai, H. Sunakawa, and A. Usui, "Defect structure in selectively grown GaN films with low threading dislocation density," Appl. Phys. Lett. **71**(16), 2259–2261 (1997).
16. D. S. Wuu, W. K. Wang, K. S. Wen, S. C. Huang, S. H. Lin, S. Y. Huang, C. F. Lin, and R. H. Horng, "Defect reduction and efficiency improvement of near-ultraviolet emitters via laterally overgrown GaN on a GaN/patterned sapphire template," Appl. Phys. Lett. **89**(16), 161105 (2006).
17. T. V. Cuong, H. S. Cheong, H. G. Kim, H. Y. Kim, C.-H. Hong, E. K. Suh, H. K. Cho, and B. H. Kong, "Enhanced light output from aligned micropit InGaN-based light emitting diodes using wet-etch sapphire patterning," Appl. Phys. Lett. **90**(13), 131107 (2007).
18. Y. J. Lee, J. M. Hwang, T. C. Hsu, M. H. Hsieh, M. J. Jou, B. J. Lee, T. C. Lu, H. C. Kuo, and S. C. Wang, "Enhancing the output power of GaN-based LEDs grown on chemical wet etching patterned sapphire substrate," IEEE Photon. Technol. Lett. **18**(10), 1152–1154 (2006).
19. Z. H. Feng, Y. D. Qi, Z. D. Lu, and K. M. Lau, "GaN-based blue light-emitting diodes grown and fabricated on patterned sapphire substrates by metalorganic vapor-phase epitaxy," J. Cryst. Growth **272**(1-4), 327–332 (2004).
20. H. C. Lin, H. H. Liu, G. Y. Lee, J. I. Chyi, C. M. Lu, C. W. Chao, T. C. Wang, C. J. Chang, and S. W. S. Chi, "Effects of lens shape on GaN grown on microlens patterned sapphire substrates by metallorganic chemical vapor deposition," J. Electrochem. Soc. **157**(3), H304–H307 (2010).
21. K. C. Shen, D. S. Wuu, C. C. Shen, S. L. Ou, and R. H. Horng, "Surface modification on wet-etched patterned sapphire substrates using plasma treatments for improved GaN crystal quality and LED performance," J. Electrochem. Soc. **158**(10), H988–H993 (2011).
22. B. W. Lin, C. Y. Hsieh, B. M. Wang, W. C. Hsu, and Y. S. Wu, "Improved performance of GaN-based LEDs by covering top c-plane of patterned sapphire substrate with oxide layer," Electrochem. Solid-State Lett. **14**(8), J48–J50 (2011).
23. W. C. Lai, C. H. Yen, Y. Y. Yang, C. K. Wang, and S. J. Chang, "GaN-based ultraviolet light emitting diodes with *ex situ* sputtered AlN nucleation layer," J. Display Technol. **9**(11), 895–899 (2013).
24. C. H. Yen, W. C. Lai, Y. Y. Yang, C. K. Wang, T. K. Ko, S. J. Hon, and S. J. Chang, "GaN-based light emitting diode with sputtered AlN nucleation layer," IEEE Photon. Technol. Lett. **24**(4), 294–296 (2012).
25. H. Heinke, V. Kirchner, S. Einfeldt, and D. Hommel, "X-ray diffraction analysis of the defect structure in epitaxial GaN," Appl. Phys. Lett. **77**(14), 2145–2147 (2000).
26. B. Heying, X. H. Wu, S. Keller, Y. Li, D. Kapolnek, B. P. Keller, S. P. DenBaar, and J. S. Speck, "Role of threading dislocation structure on the x-ray diffraction peak widths in epitaxial GaN films," Appl. Phys. Lett. **68**(5), 643–646 (1996).
27. H. Amano, N. Sawaki, I. Akasaki, and Y. Toyoda, "Metalorganic vapor phase epitaxial growth of a high quality GaN film using an AlN buffer layer," Appl. Phys. Lett. **48**(5), 353 (1986).
28. S. Watanabe, N. Yamada, M. Nagashima, Y. Ueki, C. Sasaki, Y. Tamada, T. Taguchi, and H. Kudo, "Internal quantum efficiency of highly-efficient $In_xGa_{1-x}N$-based near-ultraviolet light-emitting diodes," Appl. Phys. Lett. **83**(24), 4906–4908 (2003).
29. Y. J. Lee, C. H. Chiu, C. C. Ke, P. C. Lin, T. C. Lu, H. C. Kuo, and S. C. Wang, "Study of excitation power dependent internal quantum efficiency in InGaN/GaN LEDs grown on patterned sapphire substrate," IEEE J. Sel. Top. Quantum Electron. **15**(4), 1137–1143 (2009).
30. C.-H. Chiu, C.-C. Lin, D.-M. Deng, D.-W. Lin, J.-C. Li, Z.-Y. Li, G.-W. Shu, T.-C. Lu, J.-L. Shen, H.-C. Kuo, and K.-M. Lau, "Optical and electrical properties of GaN-based light emitting diodes grown on micro and nano-scale patterned Si substrate," IEEE J. Quantum Electron. **47**(7), 899–906 (2011).

#210923 - $15.00 USD Received 25 Apr 2014; revised 19 Jun 2014; accepted 20 Jun 2014; published 17 Jul 2014

31. M. A. Tsai, P. Yu, C. H. Chiu, H. C. Kuo, T. C. Lu, and S. H. Lin, "Self-assembled two-dimensional surface structures for beam shaping of GaN-based vertical-injection light-emitting diodes," IEEE Photon. Technol. Lett. **22**(1), 12–14 (2010).
32. Fullwave 6.1, RSoft Design Group Inc., Ossining, NY, 2008.

1. Introduction

The III-nitride GaN-based light-emitting diodes (LEDs) have been applied in many commercial products due to the wide emission spectra from green to ultraviolet (UV) [1–3]. Recently, UV-LEDs have started to attract attention in many application areas, such as photolithography, biomedicine, water purification, Hg-free back lighting source in liquid-crystal displays, high-density optical data storage, and solid-state lighting. Although the commonly used pumping source is a blue LED for white-light generation, the UV LED can be a promising contender due to its relatively high color rendering index and stable white light output [4,5]. In the past, the mismatches of lattice constants and thermal expansion coefficients between the GaN layer and the sapphire substrate have induced a high density of threading dislocations (TDs) during GaN layer growth [6]. In GaN-based materials, typical threading dislocation densities (TDDs) are as large as $10^8 - 10^{10}$ cm^{-2} [7]. Fortunately for blue LED chips, the InGaN localized states can provide a safe passage for radiative recombination and thus the luminescent efficiency of the blue InGaN quantum well (QW) LEDs is not seriously affected [8]. However, the multiple quantum well (MQW) active regions in the UV LED usually contain less indium and thus fewer localized states for carriers to by-pass the defects. This situation makes UV LEDs more sensitive to TD in the material than regular blue LEDs [9,10]. Therefore, in order to increase the output power, reducing the TDDs is one of the critical issues, especially in the short wavelength UV-LEDs. Several suggestions for the reduction of TDs have been reported, including epitaxial lateral overgrowth (ELOG) [11,12], cantilever epitaxy (CE) [13], defect selective passivation [14], microscale SiN_x or SiO_x patterned mask [15,16], and the use of patterned sapphire substrate (PSS) [17–19]. However, these methods require additional complex photolithography and etching process.

Although, the GaN layers grown by ELOG on the PSS were a common method to reduce the TDs, there were still some TDs generated at the tip of the pattern due to the coalescence of two growth fronts [20]. In order to improve the crystalline quality of GaN-based epitaxial layers at the tip of the pattern, various growth techniques have been proposed, such as Shen *et al.* who used plasma treatment to create a slightly roughened surface pattern, which not only suppressed lateral growth from the incline of the pattern, but also enhanced vertical growth from the mesa and groove of the pattern [21]. Lin *et al.* reported the preparation of a pyramid with an oxide-covered top c-plane (OPSS) [22]. The nucleation layer between the sapphire substrate and the GaN layer is the key to the dislocation density. Lai *et al*. and Yen *et al*. have employed sputtered AlN nucleation layers in LEDs and achieved improvement of crystal quality [23,24]. For the sputtering system, a higher bias voltage (200 ~400 V) is essential. Moreover, the recoiled Argon ion will damage the substrate. In this study, we demonstrate flip-chip UV-LEDs (FCUV-LEDs) with a reactive plasma deposition (RPD) AlN nucleation layer on PSS. The RPD AlN layer on PSS can potentially enhance the subsequent GaN quality via its step coverage difference which prefers the single-crystalline GaN vertical growth. Another benefit brought by the RPD AlN nucleation layer is the reduction of thermal cycle and growth time in the MOCVD system since it can be deposited before loading into the growth chamber. In the following, the electrical and optical properties of both LED samples with GaN nucleation layer and RPD AlN nucleation layer will be analyzed and compared. Finally, the mechanisms behind these results are discussed.

2. Experiments and simulations

The epitaxial InGaN/AlGaN LED structures with GaN nucleation layer and RPD AlN nucleation layer were grown on c-plane sapphire substrate by an atmospheric-pressure metal-

#210923 - $15.00 USD Received 25 Apr 2014; revised 19 Jun 2014; accepted 20 Jun 2014; published 17 Jul 2014

organic chemical vapor deposition (AP-MOCVD) system. The metal organic compounds of trimethylgallium (TMGa), trimethylaluminum (TMAl), trimethylindium (TMIn), and ammonia (NH_3) were employed as the reactant source materials for Ga, Al, In, and N, respectively. Silane and bis-cyclopentadienyl magnesium (Cp_2Mg) were used as the sources for n-type and p-type dopants, respectively. All samples were grown on a 2-in (0001) hemisphere-shape-patterned sapphire substrate (HPSS). The diameter and interval of each HPSS were 2.6 and 0.4 μm, respectively. The height was about 1.6 μm. When growing conventional UV-LEDs, a 25-nm-thick low temperature GaN nucleation layer was first deposited at 520 °C on the PSS, followed by a standard H_2 etch-back process. After depositing a 25-nm-thick low temperature GaN nucleation layer, a 3-μm-thick undoped GaN layer, and a 3-μm-thick n-type GaN layer (n-doping = 5×10^{18} cm^{-3}) were grown. On the top of the buffer layer, 10 pairs of InGaN/AlGaN MQWs were grown, followed by a 25-nm-thick p-$Al_{0.2}Ga_{0.8}N$ electron blocking layer (EBL) (p-doping = 1×10^{17} cm^{-3}) and a 50-nm-thick p-type GaN cap layer (p-doping = 5×10^{17} cm^{-3}). For comparison, the identical GaN-based LED structure was also grown on PSS with a 25-nm-thick RPD AlN nucleation layer. For the RPD process, several steps were developed to ensure the stability of deposition. The ignition of plasma with LaB6 as the cathode provides the pre-heat source for the Al target. When the Al elements are evaporated, they can react with the surrounding N_2 plasma and form AlN to deposit on the substrate. The PSS substrate was kept at 600 °C during the deposition to ensure the preferred condition of single-crystalline growth.

After the epitaxial growth, the LED mesa with an area 300 × 300 μm^2 was defined by using standard photolithography and dry etching. In addition, NiAg and CrAu metal were deposited as p-type and n-type electrodes, respectively. Using flip-chip technology, one can achieve higher LED output power since no bonding pads or wires exist on the top of the devices so that photons could be emitted freely from the substrates. A schematic diagram of the finished UV-LED is shown in Fig. 1. The LED power output was measured with a calibrating integrating sphere at room temperature.

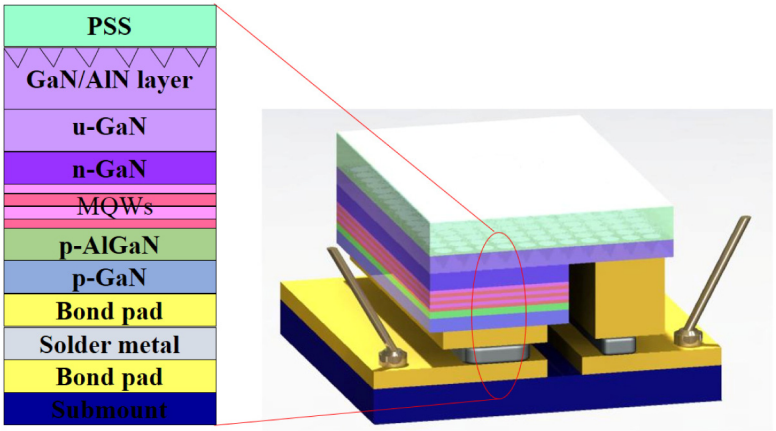

Fig. 1. Schematic of the FCUV-LEDs with different nucleation layer.

3. Results and discussions

The X-ray diffraction (HR-XRD) rocking curves of both samples for n-GaN epitaxial with the GaN nucleation layer and with the RPD AlN nucleation layer are shown in Fig. 2. The full-width at half-maximum (FWHM) for (002) planes was reduced from 298 to 229 arc sec. The FWHM for (102) planes was reduced from 353 to 263 arc sec. Heinke *et al*. reported that the XRD FWHM for (102) and (102) planes are related to edge and screw threading dislocation densities, respectively [25]. The drop in XRD FWHM indicates improved material quality.

#210923 - $15.00 USD Received 25 Apr 2014; revised 19 Jun 2014; accepted 20 Jun 2014; published 17 Jul 2014

These results indicated that the UV-LEDs grown on the RPD AlN nucleation layer has better crystalline quality than with the GaN nucleation layer.

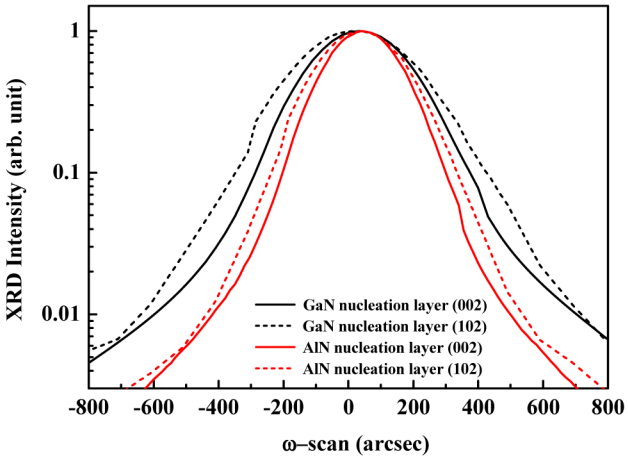

Fig. 2. X-ray rocking curves for samples with the GaN nucleation layer and with the RPD AlN nucleation layer.

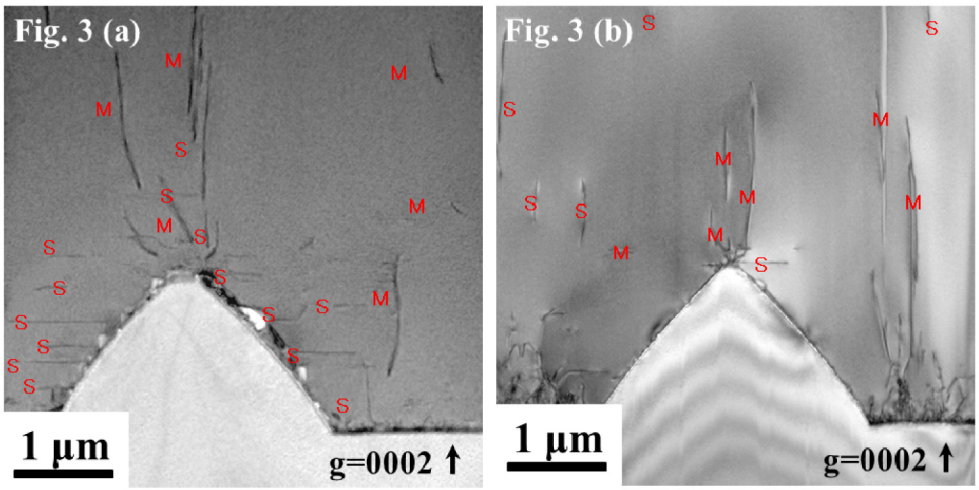

Fig. 3. Bright field cross-section TEM images of the (a) UV-LEDs with GaN nucleation layer. (b) UV-LEDs with RPD AlN nucleation layer, g = 0002. “S” indicates screw dislocation and “M” indicates mix dislocation.

To estimate the crystalline quality of GaN-based UV-LEDs, transmission electron microscopy (TEM) is utilized. Two-beam TEM images are captured to determine the nature and density of defects. Heying *et al*. pointed out that pure edge and mixed defects are visible under the g = (10-10) two-beam condition; on the other hand, pure screw and mixed defects are visible under the g = (0002) two-beam condition [26]. Figure 3 shows bright field scanning cross-section TEM images of UV-LEDs with GaN nucleation layer and RPD AlN nucleation layer. In Fig. 3(a) it is clearly observed that the tip portion of the pattern was not smooth, due to the formation of 3-D GaN islands during the growth. There exist a number of screw (S) and mix (M) dislocations on the surface of the patterns, in particular on the tip and incline region, which can be regarded as an indicator of GaN quality deterioration due to this 3-D island formation [27]. For comparison, fewer screw and mix dislocations were observed in Fig. 3(b), indicating better epitaxial quality with the RPD AlN layer. On the other hand, the

#210923 - $15.00 USD Received 25 Apr 2014; revised 19 Jun 2014; accepted 20 Jun 2014; published 17 Jul 2014

TDDs are estimated reduced from 7×10^7 cm^{-2} to 2.5×10^7 cm^{-2} at the interface between the u-GaN layers for conventional and AlN PSS devices, respectively. This confirmed the earlier statement that the crystalline quality of the GaN film was improved by RPD AlN nucleation layer growth on PSS.

Generally, the light output for the LEDs depends on their internal quantum efficiency (IQE) and light extraction efficiency (LEE). As described above, the TDDs were reduced for the LEDs with RPD AlN nucleation layers, resulting in much less non-radiative recombination, thus enhanced IQE. A general approach to evaluate the IQE for LEDs is to compare the integrated photoluminescence (PL) intensities obtained at low and room temperatures [28]. Figure 4 shows the measured IQE as a function of excitation power at 15 K and 300 K for both UV-LEDs. The efficiency is defined as the collected photon numbers divided by the injected photon numbers and normalized to the maximum efficiency achieved at low temperature. Usually the PL excitation intensity is difficult to estimate and it varies between different experiments and wafers. What we would like to do here is to convert the variable pumping intensity into the more common "carrier density" [29]. The IQE of UV-LEDs with RPD AlN nucleation layer are estimated to be 59.1% under an excitation power of 20 mW (equivalent to carrier density of 5×10^{16} cm^{-3}), corresponding to a current of 20 mA. This IQE value of the RPD sample is higher than that of the UV-LED with GaN nucleation layer (IQE~47.2%) by 25%.

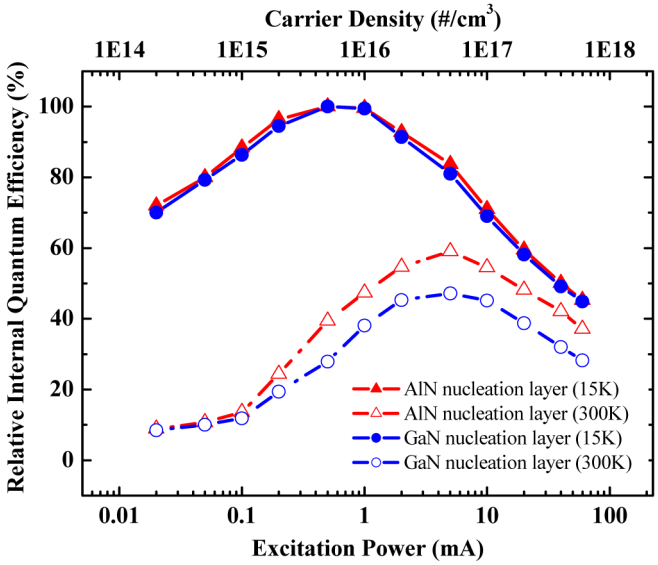

Fig. 4. Relative internal quantum efficiency as a function of excitation power for two samples.

The electroluminescence (EL) spectra, measured under the same injection current of 20 mA, were depicted in Fig. 5(a). The emission peak wavelengths for FCUV-LEDs with GaN nucleation layer and RPD AlN nucleation layer are about 372 and 373 nm, respectively. Then the finished devices were put under L-I-V measurement. Figure 5(b) presents the light power intensity as a function of injection current for both samples. From the L-I curves, the output power of FCUV-LEDs with RPD AlN nucleation layer is higher than the FCUV-LEDs with GaN nucleation layer under all current injection conditions. In particular, the light output power intensity of FCUV-LEDs with RPD AlN nucleation layer is enhanced by 30% at an injection current of 20 mA. Figure 6 shows the normalized external quantum efficiency (EQE) as a function of forward current for both LEDs. The efficiency droop, defined as $(\eta_{peak} - \eta_{100\ mA})/\eta_{peak}$, is reduced from 30% in FCUV-LEDs with GaN nucleation layer to 20% in

#210923 - $15.00 USD Received 25 Apr 2014; revised 19 Jun 2014; accepted 20 Jun 2014; published 17 Jul 2014

UV-LEDs with RPD AlN nucleation layer. This improvement could be mainly attributed to the better crystal quality, and also the reduction of dislocations of InGaN/AlGaN MQWs [30].

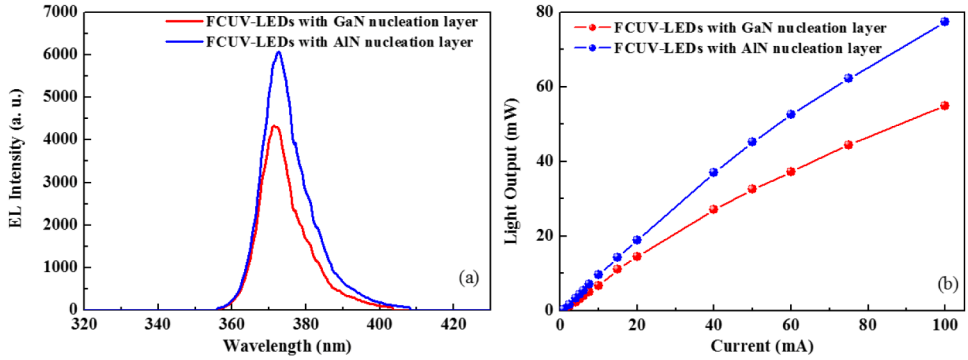

Fig. 5. (a) Electro-luminescence (EL) spectrum under 20 mA injection current of both samples. (b) Light output of both samples.

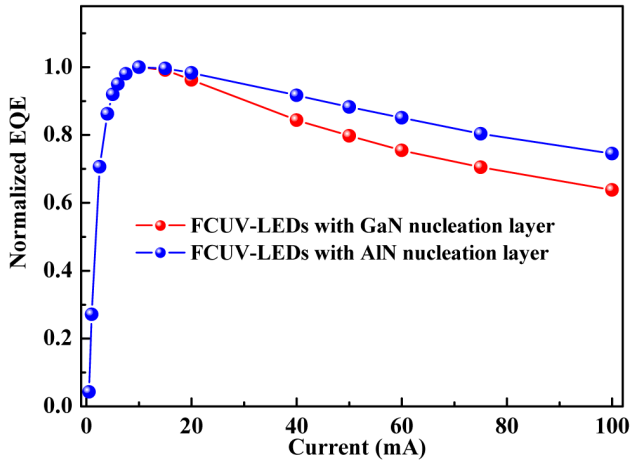

Fig. 6. EQE as a function of current for two samples.

On the other hand, the internal absorption of the GaN nucleation layer is higher, especially for UV-LEDs. Therefore, we still need to quantify how much improvement of the L-I is coming from the better light extraction scheme due to the RPD AlN nucleation layer. A 3-D finite difference time domain (FDTD) simulation was applied to calculate the LEE of the LEDs using the FullWAVETM program [31]. A 5 × 5 periodic triangle pyramidal array PSS with a height of 6.22 μm was employed in the simulation structure. The light sources are composed of 15 dipole illuminators placed 0.22 μm below the detector of the simulated device [32]. The calculated electric-field distributions with GaN nucleation layer and RPD AlN nucleation layer are shown in Fig. 7(a). As can be seen in the figure, the light intensity of FCUV-LEDs with RPD AlN nucleation layer is higher than that of FCUV-LEDs with GaN nucleation layer at the monitor. The corresponding normalized light output as a function of the simulation time is calculated and plotted in Fig. 7(b), and the enhancement of extra light scattering is defined as the ratio of steady-state light output of FCUV-LEDs with RPD AlN nucleation layer to that of UV-LEDs with GaN nucleation layer. From the simulated results, light output of the UV-LEDs with an RPD AlN nucleation layer is around 1.04 times higher than that of the UV-LEDs with GaN nucleation layer. Combining with the previous PL IQE measurement, we can see a total enhancement of 29.3% (4.3% from LEE and 25% from IQE)

#210923 - $15.00 USD Received 25 Apr 2014; revised 19 Jun 2014; accepted 20 Jun 2014; published 17 Jul 2014

when we compare the result to a conventional LED structure. The actual increase in power output of the LED, which is 30%, is close to the prediction.

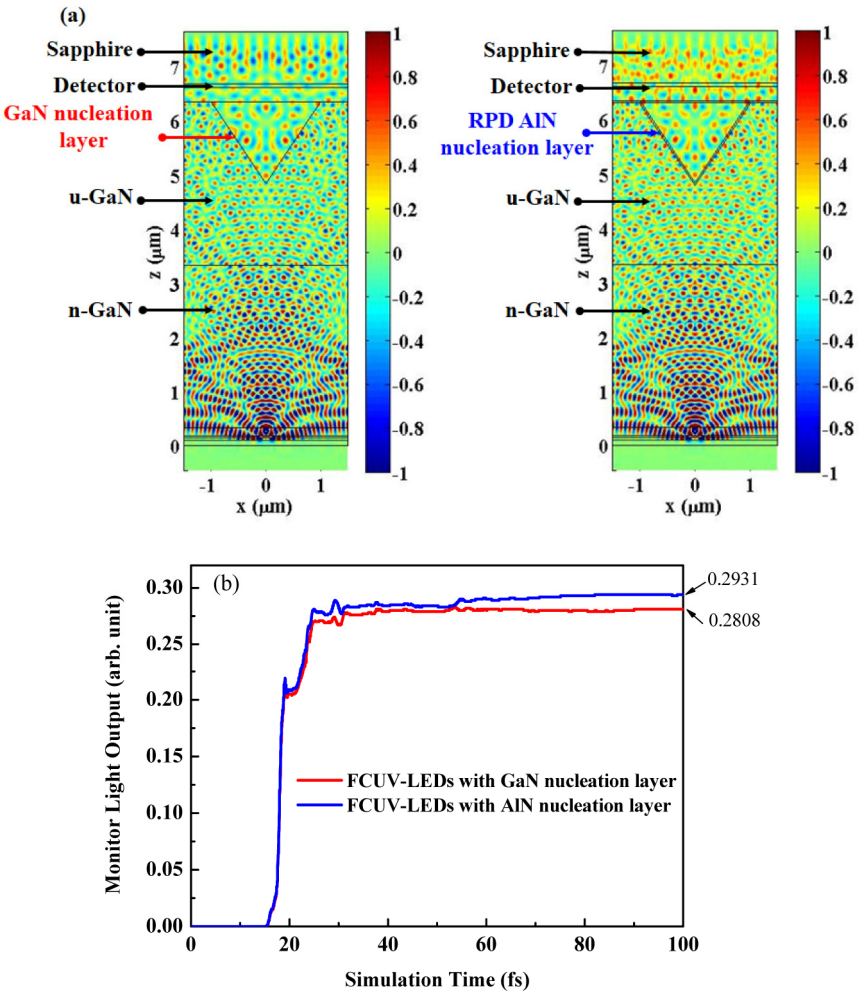

Fig. 7. (a) 3D-FDTD of the calculated electric-field distribution for both samples. (b) Monitor light output power as functions of the simulation time for both samples.

4. Conclusion

In summary, we have demonstrated the electro-optical characteristics of GaN-based UV-LEDs with an RPD AlN nucleation layer. From the XRD measurement, the TDDs were reduced effectively by the RPD AlN nucleation layer and result in the improvement of crystal quality for the GaN-based UV-LEDs. From the cross-section TEM images, it can be observed that the tip and incline portion of the pattern was smooth using an RPD AlN nucleation layer. Meanwhile, the relative light output power was found to be enhanced by a factor of approximately 30% at an injection current of 20 mA. With power-dependent PL measurement and 3-D FDTD simulation, we can estimate that the enhancement brought by each factor (IQE and LEE) should be 25% and 4.3%, respectively, and this is close to what we observed in L-I measurements (30% at 20 mA).

#210923 - $15.00 USD Received 25 Apr 2014; revised 19 Jun 2014; accepted 20 Jun 2014; published 17 Jul 2014

Acknowledgment

This work was funded by the National Science Council in Taiwan under grant number, NSC-103-3113-E-009 –001-CC2.

#210923 - $15.00 USD Received 25 Apr 2014; revised 19 Jun 2014; accepted 20 Jun 2014; published 17 Jul 2014